Outage-based LDPC Code Design for SC/MMSE Turbo-Equalization

Rainer Wohlgenannt
Austria*micro*systems AG
Schloss Premstaetten, A-8141 Premstaetten, Austria
rainer.wohlgenannt@austriamicrosystems.com

Kimmo Kansanen, Djordje Tujkovic, Tad Matsumoto
University of Oulu
POB 4500, FIN-90014 University of Oulu, Finland
kimmo.kansanen@ee.oulu.fi

***Abstract*— A semi-analytical EXIT chart analysis approach is presented to perform code design of low-density parity-check (LDPC) codes with a frequency-domain SC/MMSE turbo equalizer. The approach utilizes the equivalent channel assumption at the equalizer output to analytically compute the equalizer output mutual information. The analysis is used to compute the EXIT functions of the receiver for a sample set of random channel realizations. LDPC code design is then performed to match the channel code to the random convergence properties of the equalizer to obtain a desired outage probability. Substantial performance improvement is achieved with the code design compared to a standard regular LDPC code. Target block error probability is not reached, which is considered to be the result of some of the approximations made in the analysis and code design.**

I. INTRODUCTION

The turbo principle has provided with means to implement powerful equalization with reasonable complexity. As a receiver technique it has given new momentum for broadband single-carrier systems that require receivers with strong equalizers. The turbo principle requires that soft information is exchanged between the equalizer and the channel decoder, and, thus, the convergence properties and the performance of the receiver depends on the properties of both the equalizer and the channel decoder, i.e. the channel code. Given this strong dependence, studies have been made of the convergence properties of turbo equalization given some known channel codes, but little work has focused on developing new channel codes with the iterative receiver in mind. One of the reasons is that the convergence properties of turbo equalizers have so far been studied in a few chosen, although illustrative, channel scenarios[1][2], whereas a more generic convergence analysis in random channels remains undone despite some efforts to that direction[3].

In this paper we propose a method for designing codes for systems employing turbo equalization. We study the convergence of the SC/MMSE frequency-domain turbo equalizer and propose a computationally efficient method to obtain the convergence characteristic (EXIT chart) of the equalizer in a manner similar to [4]. The method is used to compute the EXIT charts of the receiver for a sample set of random channels generated with a simple channel model. The charts are then used in a code design procedure that seeks to achieve a *convergence outage*. An irregular LDPC code is designed to realize a design EXIT characteristic that results in unsuccesfull convergence in a given (P_{out}) percentage of channel realizations. The designed code is in other words matched to reach the design outage in the channel with given parameters.

This work was performed during the employment at University of Oulu, Centre for Wireless Communications from 1.2. to 30.4.2004. This work has been supported by Finnish Defence Forces, National Technology Agency of Finland (Tekes), Nokia, Elektrobit Ltd. and Instrumentointi Ltd.

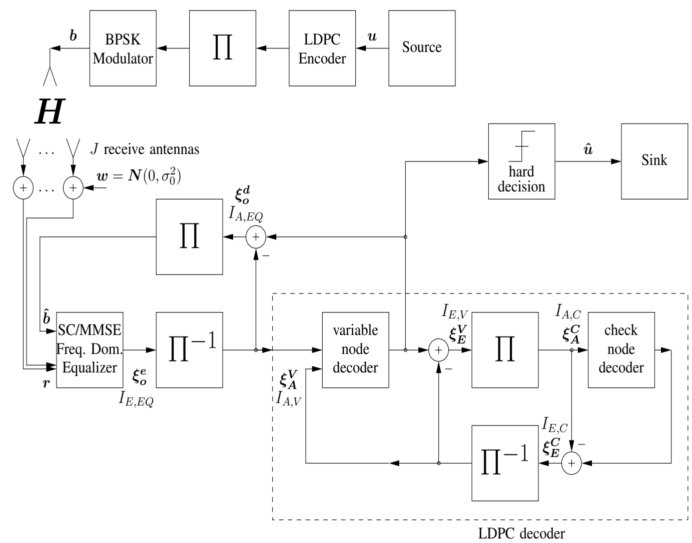

Fig. 1. System Model

The paper is organized as follows. The SIMO system model is presented in Section II. The SC/MMSE block turbo equalizer is presented in Section III and its frequency-domain implementation in Section IV. The convergence analysis based on EXIT charts is shortly reviewed in Section V and applied to the equalizer in Section VI. The proposed code design is presented in Section VII. The designed codes are tested with simulations in Section VIII, and the paper concludes with conclusions.

II. SYSTEM MODEL

In the following, vectors are marked with bold lowercase, matrices with bold uppercase notation. An indexed matrix or vector, i.e. $r(\dot{})$ denotes a submatrix or -vector. An estimate of a variable is denoted by $\hat{()}$.

0-7803-8887-9/05/$20.00 (c)2005 IEEE

The information bits are arranged into a vector $\mathbf{u}$ of length k. The information vector $\mathbf{u}$ is encoded with an LDPC encoder of rate $R = \frac{k}{N}$, interleaved and BPSK modulated which yields the symbol vector

$$\mathbf{b} \quad = \quad [b(1), \ldots, b(n), \ldots, b(N)]^{\mathrm{T}}, \tag{1}$$

where N is the length of the transmission block. The space-time multipath channel matrix $\mathbf{H}$ with L separable multipaths and J receiver antennas is given as

$$\mathbf{H} \quad = \quad \left[\mathbf{H}_1^{\mathrm{T}}, \ldots, \mathbf{H}_j^{\mathrm{T}}, \ldots, \mathbf{H}_J^{\mathrm{T}}\right]^{\mathrm{T}} \tag{2}$$

$$\mathbf{H}_j \quad = \quad \left[\bar{\mathbf{h}}_j(1), \ldots, \bar{\mathbf{h}}_j(n), \ldots, \bar{\mathbf{h}}_j(N)\right], \tag{3}$$

where $\bar{\mathbf{h}}_j(n) = \left[\mathbf{0}_{n-1}^{\mathrm{T}}, \mathbf{h}_j^{\mathrm{T}}(n), \mathbf{0}_{N-n+1}^{\mathrm{T}}\right]^{\mathrm{T}}$ incorporates the channel multipath response between the transmitter and the receive antenna j at time n

$$\mathbf{h}_j(n) \quad = \quad \left[\mathbf{h}_{j,1}^{\mathrm{T}}(n), \ldots, \mathbf{h}_{j,l}^{\mathrm{T}}(n), \ldots, \mathbf{h}_{j,L}^{\mathrm{T}}(n)\right]^{\mathrm{T}}. \tag{4}$$

In (4) $\mathbf{0}_q$ denotes an all-zeros vector of length q. For convenience, we also define the channel experienced by a single transmitted symbol as

$$\mathbf{h}(n) = \left[\bar{\mathbf{h}}_1^{\mathrm{T}}(n), \ldots, \bar{\mathbf{h}}_j^{\mathrm{T}}(n), \ldots, \bar{\mathbf{h}}_J^{\mathrm{T}}(n)\right]^{\mathrm{T}}. \tag{5}$$

When the symbols (1) pass through the frequency selective channel, the received signal, embedded in complex Gaussian noise $\mathbf{w}$ with variance σ_0^2, is given as

$$\mathbf{r} \quad = \quad \mathbf{H}\mathbf{b} + \mathbf{w}. \tag{6}$$

III. Block SC/MMSE MIMO Turbo Equaliser

The iterative receiver consists of a soft-in-soft-out (SISO) SC/MMSE equalizer and the LDPC channel decoder. The equalizer computes the extrinsic log-likelihood ratios (LLRs) of encoded symbols as

$$\xi_o^e(n) = \frac{4\Re\{z(n)\}}{1 - \mu(n)}, \tag{7}$$

where the equalizer filter output $z(n)$ is assumed to be Gaussian distributed, with mean $\mu(n)$. The variables $z(n)$ and $\mu(n)$ are computed through the MMSE solution of a interference cancelled received signal as follows. From the feedback, the *soft* symbol estimates

$$\hat{b}(n) \quad = \quad \tanh\left(\frac{\xi_o^d(n)}{2}\right), \tag{8}$$

are obtained for each $k = 1 \ldots K$ and $n = 1 \ldots N$, where $\xi_o^d(n)$ is the LLR output of the LDPC decoder. The symbol estimates $\hat{b}(n)$ are then utilized in the cancellation of known signal components from the received signal to provide the residual

$$\tilde{\mathbf{r}} \quad = \quad \mathbf{r} - \mathbf{H}\hat{\mathbf{b}}. \tag{9}$$

Similar to [5], an MMSE minimization problem

$$\arg\min_{\mathbf{u}^{\mathrm{H}}} \left| b(n) - \mathbf{u}^{\mathrm{H}}\left(\tilde{\mathbf{r}} + \mathbf{h}(n)\hat{b}(n)\right)\right|^2 \tag{10}$$

is then solved to compute the filter taps $\mathbf{u}^{\mathrm{H}}$ for the interference cancelled signal combined with the desired symbol information. Notice, the filter $\mathbf{u}^{\mathrm{H}}$ is defined over the received frame. The filter output is given as

$$z(n) = \mathbf{u}^{\mathrm{H}}\left(\tilde{\mathbf{r}} + \mathbf{h}(n)\hat{b}(n)\right), \tag{11}$$

where

$$\mathbf{u}^{\mathrm{H}} \quad = \quad \mathbf{h}^{\mathrm{H}}(n)\boldsymbol{\Sigma}^{-1}(n), \tag{12}$$

$$\boldsymbol{\Sigma}(n) \quad = \quad \boldsymbol{\Sigma} + \mathbf{h}(n)\left|\hat{b}(n)\right|^2 \mathbf{h}^{\mathrm{H}}(n), \tag{13}$$

$$\boldsymbol{\Sigma} \quad = \quad \mathbf{H}\boldsymbol{\Lambda}\mathbf{H}^{\mathrm{H}} + \sigma_0^2\mathbf{I}, \tag{14}$$

$$\boldsymbol{\Lambda} \quad = \quad \operatorname{diag}\left\{1 - \hat{\mathbf{b}}^2\right\}. \tag{15}$$

To compute the symbol LLR $\xi_o^e(n)$ as in Eq. (7), the equalizer output is approximated as Gaussian distributed $z(n) \sim N(\mu(n)b(n), \nu(n))$ with

$$\mu(n) \quad = \quad \mathbf{h}^{\mathrm{H}}(n)\boldsymbol{\Sigma}^{-1}(n)\mathbf{h}(n), \tag{16}$$

$$\nu(n) \quad = \quad \mu(n)\left(1 - \mu(n)\right). \tag{17}$$

With the aid of the matrix inversion lemma, we can reformulate (11) and (16) as

$$z(n) \quad = \quad \beta(n)\left(\alpha(n)\hat{b}(n) + \mathbf{h}^{\mathrm{H}}(n)\boldsymbol{\Sigma}^{-1}\tilde{\mathbf{r}}\right) \tag{18}$$

$$\mu(n) \quad = \quad \alpha(n)\beta(n), \tag{19}$$

where

$$\alpha(n) \quad = \quad \mathbf{h}^{\mathrm{H}}(n)\boldsymbol{\Sigma}^{-1}\mathbf{h}(n) \tag{20}$$

$$\beta(n) \quad = \quad \left(1 + \alpha(n)\left|\hat{b}(n)\right|^2\right)^{-1}. \tag{21}$$

To extend the algorithm to the whole frame, we denote

$$\mathbf{D} \quad = \quad \operatorname{diag}\left\{\mathbf{H}^{\mathrm{H}}\left(\mathbf{H}\boldsymbol{\Lambda}\mathbf{H}^{\mathrm{H}} + \sigma_0^2\mathbf{I}\right)^{-1}\mathbf{H}\right\} \tag{22}$$

$$\mathbf{B} \quad = \quad \operatorname{diag}\{\beta(n)\}. \tag{23}$$

The equalizer output vector $\mathbf{z}$ for the frame can then be expressed as

$$\mathbf{z} \quad = \quad (\mathbf{I} + \mathbf{B}\mathbf{D})^{-1}\left(\mathbf{D}\hat{\mathbf{b}} + \mathbf{H}^{\mathrm{H}}\boldsymbol{\Sigma}^{-1}\tilde{\mathbf{r}}\right). \tag{24}$$

IV. Frequency-domain Equalizer

If a time-domain linear filter has a large number of taps, it can be computationally more efficient to implement it in frequency domain. A similar approach for frequency-domain MIMO turbo equalization to what is presented here was proposed in [6]. For a straightforward application of frequency-domain filtering, we assume the transmission is cyclic, so that the first P tranmitted symbols are repeated at the end or the frame. Given the channel remains static over the frame, the channel matrix appears block-circulant to the receiver, and a DFT operation can be utilized at the receiver for the fourier transformation. A $N \times N$ DFT matrix operator $\mathbf{F}$ with $[\mathbf{F}]_{i,j} = N^{-\frac{1}{2}} e^{-\jmath\frac{2\pi}{N}(i-1)(j-1)}, \jmath = \sqrt{-1}$ is defined for Fourier transformation. Next, we express the block-circulant channel matrix as the product

$$\mathbf{H} = \mathbf{F}_J^{\mathrm{H}} \mathbf{\Xi} \mathbf{F}, \tag{25}$$

where we utilize the block-Fourier matrix

$$\mathbf{F_J} = \mathbf{I}_J \otimes \mathbf{F}, \tag{26}$$

where $\mathbf{I}_J$ is an identity matrix of dimension J and $\otimes$ denotes the Kronecker product. The block-diagonal frequency-domain channel matrix can then be expressed as

$$\mathbf{\Xi} = \left[\mathbf{\Xi}_1^{\mathrm{T}}, \ldots, \mathbf{\Xi}_j^{\mathrm{T}}, \ldots, \mathbf{\Xi}_J^{\mathrm{T}}\right]^{\mathrm{T}} \tag{27}$$

$$\mathbf{\Xi}_j = \operatorname{diag}\left\{\tilde{h}_j(1), \ldots, \tilde{h}_j(f), \ldots, \tilde{h}_j(N)\right\}, \tag{28}$$

where $f = 1 \ldots N_f$ enumerates the frequency bins. If we now define the frequency domain covariance matrix

$$\mathbf{\Gamma} = \mathbf{\Xi}^{\mathrm{H}} \left(\mathbf{\Xi F \Lambda F^{\mathrm{H}} \Xi^{\mathrm{H}}} + \sigma_0^2 \mathbf{I}\right)^{-1} \mathbf{\Xi}. \tag{29}$$

The elements on the diagonal of $\mathbf{\Lambda}$ are i.i.d. and the frequency-domain covariance matrix of the feedback soft estimates

$$\mathbf{\Delta} = \mathbf{F}_N \mathbf{\Lambda} \mathbf{F}_N \tag{30}$$

$$= \operatorname{circ}\{\mathbf{F}_N \boldsymbol{\lambda}\} \tag{31}$$

is a circulant matrix with the Fourier transformation of the diagonal of $\mathbf{\Lambda}$, $\boldsymbol{\lambda} = [\lambda_1, \ldots, \lambda_n, \ldots, \lambda_N]^{\mathrm{T}}$ on the first column. The diagonal of $\mathbf{\Delta}$ is then constant with the value

$$\bar{\lambda} = \frac{1}{N} \sum_{n=1}^{N} \lambda_n. \tag{32}$$

When the diagonal is large compared to the off-diagonal elements, the matrix can be approximated with the constant diagonal matrix

$$\mathbf{\Delta} \approx \bar{\lambda} \mathbf{I}. \tag{33}$$

Now we can approximate (29) with

$$\mathbf{\Gamma} \approx \mathbf{\Xi}^{\mathrm{H}} \left(\bar{\lambda} \mathbf{\Xi \Xi}^{\mathrm{H}} + \sigma_0^2 \mathbf{I}\right)^{-1} \mathbf{\Xi}, \tag{34}$$

and (22) with

$$\mathbf{D} \approx \operatorname{diag}\left\{\mathbf{F}_N^{\mathrm{H}} \tilde{\mathbf{\Gamma}} \mathbf{F}_N\right\}. \tag{35}$$

When we make the definitions

$$\gamma = N^{-1} \mathbf{tr}\left\{\tilde{\mathbf{\Gamma}}\right\} \tag{36}$$

$$\delta = \mathrm{E}\left[\hat{b}^2(n)\right], \tag{37}$$

we can express the approximate frequency-domain filtering equation as

$$\mathbf{z}_a = (1 + \delta\gamma)^{-1} \times \tag{38}$$

$$\left(\gamma \hat{\mathbf{b}} + \mathbf{F}_N^{\mathrm{H}} \mathbf{\Xi}^{\mathrm{H}} \left(\bar{\lambda} \mathbf{\Xi \Xi}^{\mathrm{H}} + \sigma_0^2 \mathbf{I}\right)^{-1} \mathbf{F}_J \tilde{\mathbf{r}}\right). \tag{39}$$

The equalizer output can now be approximated as the output of an equivalent Gaussian channel with the pdf $\mathbf{z}_a \sim N(\nu \mathbf{b}, \nu(1-\nu))$, where

$$\tilde{\mu} = \gamma (1 + \delta\gamma)^{-1}. \tag{40}$$

The likelihoods computed with (7) are approximately distributed according to $\xi_o^e \sim N\left(\frac{4\tilde{\mu}\mathbf{b}}{1-\tilde{\mu}}, \frac{8\tilde{\mu}\mathbf{b}}{1-\tilde{\mu}}\right)$. We note that the mutual information I at the equalizer output can be computed by obtaining δ from (37) with the aid of (8) and a prior pdf for the extrinsic information provided by the decoder, and then solving for γ and $\tilde{\mu}$ from (34) and (40).

V. Extrinsic Information Transfer (EXIT) Charts

EXIT Charts[7] show the development over iterations of the averaged mutual information I between the binary digits of the sent vector $\boldsymbol{b}$ and the extrinsic LLRs at various positions inside the receiver. With the first index of I, we denote whether the mutual information I is considered as an input (a priori information) I_A or as an ouput (extrinsic information) I_E. The second index denotes the block under consideration ($V \ldots$ variable node decoder, $C \ldots$ check node decoder, $EQ \ldots$ equalizer). For example, the a priori mutual information at the input of the equalizer computes as

$$I_{A,EQ} = \sum_{n=1}^{N} I\left(b(n); \xi_o^d(n)\right). \tag{41}$$

Under the assumption that the LLRs conditioned on the elements of the binary input vector $\mathbf{b}$ are Gaussian distributed and fulfill the symmetry condition (mean and variance are connected as $\mu = \frac{\sigma^2}{2}$), the mutual information can be computed with the $J()$ -function as

$$I_{A,EQ} := J(\sigma_{\xi_o^d}), \tag{42}$$

$$\sigma_{\xi_o^d} := J^{-1}(I_{A,EQ}), \tag{43}$$

where $\sigma^2_{\xi_o^d}$ is the variance of the LLRs $\boldsymbol{\xi_o^d}$. The inverse function $J^{-1}()$ is used to determine the variance of the LLRs from the corresponding mutual information. Similarly, as in Eq. (41) the *a priori* mutual information at at the input of the variable node decoder $I_{A,V}$ and the mutual information at the in- and output of the check node decoder $I_{A,C}, I_{E,C}$ and the equalizer $I_{A,EQ}, I_{E,EQ}$ can be computed.

This leads to the definition of EXIT functions for the variable node decoder (VND) $f_V()$, check node decoder (CND) $f_C()$ and and the equalizer $f_{EQ}()$ which show how the corresponding module amplifies or attenuates mutual information

$$I_{E,V} := f_V(I_{A,V}), \tag{44}$$

$$I_{E,C} := f_C(I_{A,C}), \tag{45}$$

$$I_{E,EQ} := f_{EQ}(I_{A,EQ}). \tag{46}$$

The EXIT functions of the VND and the CND depend on the LDPC code properties and the average SNR of the VND input and are well known under the assumption of Gaussian distributed LLRs [8]. As a specialty, the EXIT function of the equalizer $f_{EQ}()$ depends on the concrete channel realization $\boldsymbol{H}$ and instantaneous channel SNR given by

$$\frac{E_b}{N_0} = \frac{RJ}{2\sigma_0^2}, \tag{47}$$

and is determined in the following section.

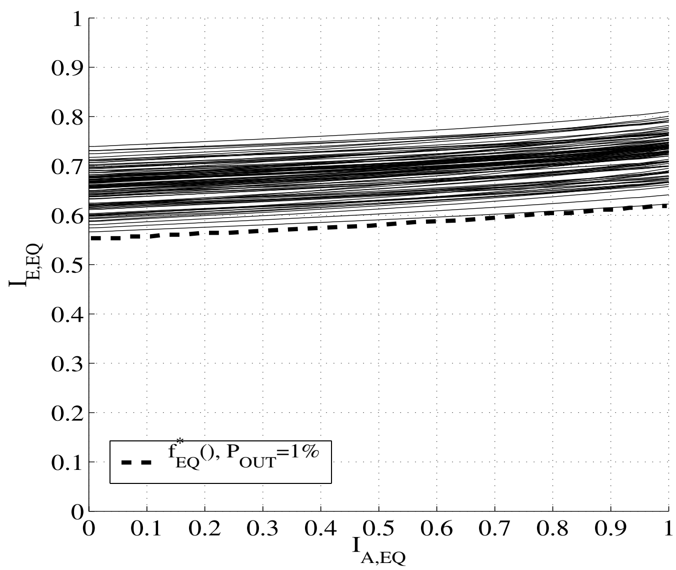

Fig. 2. Equalizer EXIT functions $f_{EQ}()$ and outage based equalizer EXIT function $f^*_{EQ}()$, $E_b/N_0 = 0$dB.

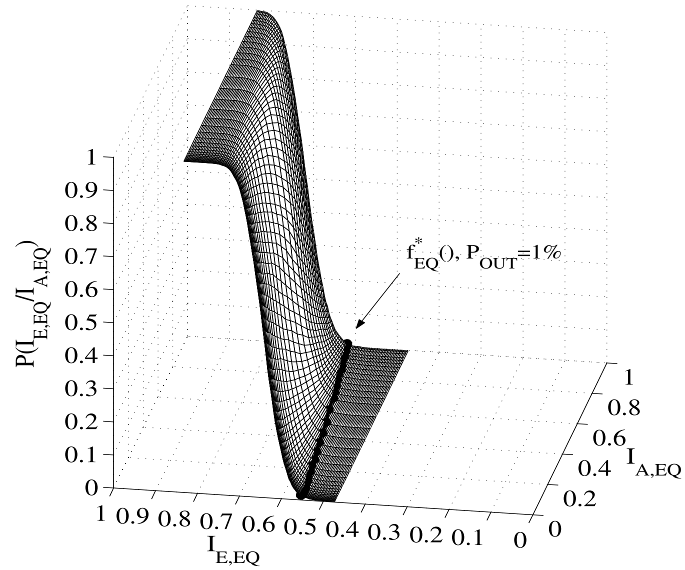

Fig. 3. Cdf of equalizer EXIT functions $f_{EQ}()$ and outage based equalizer EXIT function $f^*_{EQ}()$, $E_b/N_0 = 0$dB.

VI. EXIT FUNCTION OF THE EQUALIZER

By the semianalytical approach given in Section IV, we obtain the different transfer functions $f_{EQ}()$ of the equalizer by varying the variance of the input LLRs $\boldsymbol{\xi}_{\boldsymbol{o}}^{\boldsymbol{d}}$, performing the computations according to Eq. (8) and (40), and computing the variance of the output LLRs $\boldsymbol{\xi}_{\boldsymbol{o}}^{\boldsymbol{e}}$. The $J()$-function (Eq. (42)) is used to compute the mutual information $I_{A,EQ}$ and $I_{E,EQ}$ from the variance of the LLRs $\boldsymbol{\xi}_{\boldsymbol{o}}^{\boldsymbol{d}}$ and $\boldsymbol{\xi}_{\boldsymbol{o}}^{\boldsymbol{e}}$. Observe, the transfer function is parametrized by the realizations of the channel matrix $\boldsymbol{H}$ as shown in Fig. 2.

For pragmatic reasons we make the assumption that the equalizer transfer functions $f_{EQ}()$ are parallel with regard to different channel realizations. This is relatively realistic in channels with a high diversity order for a majority of the channel realizations. Assume, we pick one particular curve $f^*_{EQ}()$ out of the bunch of curves and guarantee a successful decoding behavior for this particular curve by optimizing the LDPC code properties. Then, a successful decoding process will also be guaranteed for all curves which lie above $f^*_{EQ}()$ as they provide a higher output mutual information $I_{E,EQ}$ for a certain input mutual information $I_{A,EQ}$. The curve $f^*_{EQ}()$ is determined by crossing a plane parallel to the x, y-plane in a certain z-elevation $P(I_{E,EQ}|I_{A,EQ}) = P_{OUT}$ with the cumulative distribution function (cdf) $P(I_{E,EQ}|I_{A,EQ})$ of the equalizer EXIT functions (Fig. 3). Only a guaranteed and arbitrarily determinable percentage of curves P_{OUT} which lie below (or intersect with) $f^*_{EQ}()$ will lead to a unsuccessful decoding process and, therefore, to a frame error.

VII. COMBINED EXIT FUNCTION AND CODE DESIGN

For LDPC code design, we consider the worst case scenario where only one iteration inside the LDPC decoder (between VND and CND) is performed and then an additional iteration between LDPC decoder and equalizer is needed to process further (Fig. 1). So, we compute an overall EXIT function $f_{VEQ}()$ which represents the combined functionality of the VND and the equalizer similarly as in [8]

$$\begin{aligned} I_{E,V} &= f_{VEQ}(I_{A,V}) \\ &= f_V\left(J\left(\sqrt{\left(J^{-1}\left(I_{E,EQ}\right)\right)^2 + \left(J^{-1}\left(I_{A,V}\right)\right)^2}\right)\right), \end{aligned} \tag{48}$$

with

$$I_{E,EQ} = f_{EQ}(f_V(I_{A,V})), \tag{49}$$

where we used the fact that the VND adds the LLRs coming from the equalizer and the CND. Therefore, we added the variances of the corresponding LLRs and used the $J^{-1}()$-function from Eq. (43) to compute them.

LDPC code design then consists of matching the combined $f_{VEQ}()$ curve to the $f_C()$ curve without any intersection for the lowest possible E_b/N_0 (which corresponds to the so called threshold value $E_b/{N_0}^*$) by optimizing the degree distribution of the LDPC Codes as in [8]. With a_{v_i} we denote the percentage of variable *nodes* with degree d_{v_i}.

VIII. NUMERICAL RESULTS

In our simulations, we considered a channel with a power delay profile of 32 independent and equally distributed channel taps and $J = 2$ receive antennas. We choose to have check regular LDPC codes with only one check node degree d_c. The EXIT chart of the optimized code *opt1* with $R = 0.5$ for the given channel is shown in Fig. 4. Observe, the axis for the CND EXIT curve $f_C()$ are swapped and the dotted curve shows the amplified difference of the combined EXIT function $f_{VEQ}()$ and the CND EXIT $f_C()$ curve and is a measure for the fitting of the two curves. The degree distribution

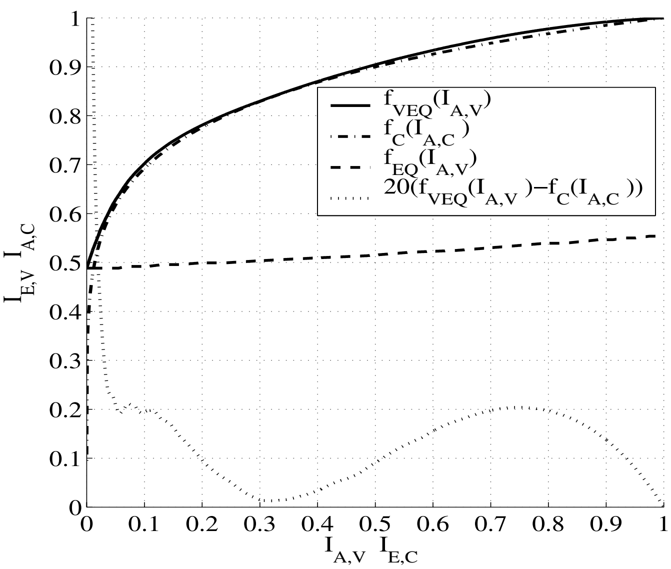

Fig. 4. EXIT chart of optimized code *opt1* for $E_b/N_0 = 2.0$dB.

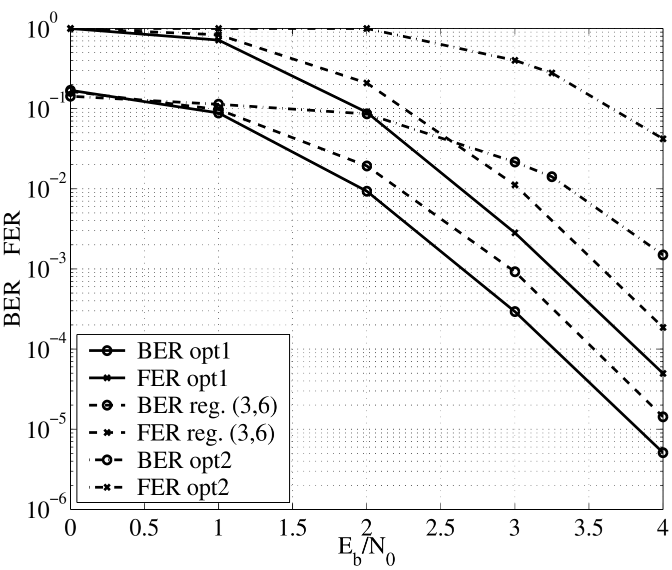

Fig. 5. Bit (BER) and frame error rates (FER) of optimized LDPC codes.

of optimized codes with a certain code rate R and outage probability P_{OUT} (or, equivalently, frame error rate) for the minimum necessary $\frac{E_b}{N_0}^*$ (threshold value) is given in Tab. I. For comparison, we give the parameters of the regular $(3, 6)$ $(R = 0.5)$ standard LDPC code. The code *opt2* was optimized to achieve the highest possible rate of $R = 0.75$ for an outage of $P_{OUT} = 0.1$ and given average channel $\frac{E_b}{N_0} = 3.25$ dB.

In Fig. 5 bit error (BER) and frame error (FER) simulation results of the codes of Tab. I are given. According to the outage based design approach we expect that the codes show a frame error rate which equals P_{OUT} at the threshold value $\frac{E_b}{N_0}^*$. For the code *opt1* the simulated threshold value equals 2.65 dB instead of 2.00 dB ($\Delta = 0.65$ dB), for the regular *(3,6)* Code

TABLE I

DEGREE DISTRIBUTION (NODE PERSPECTIVE) OF CODES.

Name	P_{OUT}	R	d_c	d_{v_1}	d_{v_2}	d_{v_3}	a_{v_1}	a_{v_2}	a_{v_3}	$\frac{E_b}{N_0}^*$ in dB
opt1	0.01	0.50	8	20	3	2	0.07	0.74	0.19	2.00
(3,6)	0.01	0.50	6	3	-	-	1.00	-	-	2.75
opt2	0.10	0.75	12	14	3	2	0.04	0.44	0.52	3.25

$\frac{E_b}{N_0}^* = 3.00$ dB instead of 2.75 dB ($\Delta = 0.25$ dB) and for *opt2* $\frac{E_b}{N_0}^* = 2.65$ dB instead of 3.25 dB ($\Delta = 0.40$ dB).

IX. CONCLUSIONS

We have introduced a new design concept of LDPC codes with EXIT charts based on outage probability. The EXIT charts for the turbo equalizer are obtained by a computationally efficient semianalytical procedure that enables the study of random channel realizations. Simulation results show that improvements are possible and an adaption of code rates to channel $\frac{E_b}{N_0}$ is feasible. However, performance lies below expectations because of the following reasons:

- The Gaussian assumption is not totally fulfilled. Particularly irregular codes with high variable node degrees cause high magnitudes of the LLRs which is is in contrary to the Gaussian assumption.
- The EXIT analysis of the equalizer is optimistic when the prior information is low. This will result in higher threshold than the design target.
- Due to the short block length, the designed performance is not achieved at the threshold value $\frac{E_b}{N_0}^*$ but at higher values of $\frac{E_b}{N_0}$. Simulation results show that code design with EXIT charts lead to performance improvements. However, the optimized codes show the improvements several decades above $\frac{E_b}{N_0}^*$ and can even perform poorer than unoptimized codes at $\frac{E_b}{N_0}^*$.

REFERENCES

[1] M. Tüchler, R. Koetter, and A. C. Singer, "Turbo equalisation: Principles and new results," *IEEE Trans. Commun.*, vol. 50, no. 5, pp. 754–767, May 2002.

[2] A. Dejonghe and L. Vandendorpe, "Turbo-equalisation for multilevel modulation: an efficient low-complexity scheme," in *Proc. IEEE Int. Conf. Commun.*, New York, USA, Apr. 28–May 2 2002, vol. 3, pp. 1863–1867.

[3] A. Roumy, A.J Grant, I. Fijalkow, P.D Alexander, and D. Pirez, "Turbo equalization: Convergence analysis," in *Proc. IEEE Int. Conf. Acoust., Speech, Signal Processing*, New Jersey, USA, 2001, vol. 4, pp. 2645–2648.

[4] C. Hermosilla and L. Szczecinski, "Performance evaluation of linear turbo receivers using analytical EXIT functions," in *Proc. IEEE Int. Symp. Pers., Indoor, Mobile Radio Commun.*, Barcelona, Spain, Sept.5–8 2004.

[5] D. Reynolds and X. Wang, "Low-complexity turbo-equalization for diversity channels," *Signal Processing, Elsevier Science Publishers*, vol. 81, no. 5, pp. 989–995, May 2000.

[6] M.S.Yee, M.Sandell, and Y.Sun, "Comparison study of single-carrier and multi-carrier modulation using iterative based receiver for MIMO system," in *Proc. IEEE Veh. Technol. Conf.*, Milan, Italy, May 17–19 2004.

[7] S. ten Brink, "Convergence behavior of iteratively decoded parallel concatenated codes," *IEEE Trans. Commun.*, vol. 49, no. 10, pp. 1727–1737, Oct. 2001.

[8] S. ten Brink, G. Kramer, and A. Ashikhmin, "Design of low-density parity-check codes for modulation and detection," *IEEE Trans. Commun.*, vol. 52, no. 4, pp. 670–678, June 2004.